Leptogenesis and Gravitino Dark Matter

Wilfried Buchmüller

Deutsches Elektronen-Synchroton DESY, 22607 Hamburg, Germany

arXiv:hep-ph/0611368 v1 29 Nov 2006

Abstract. We study implications of thermal leptogenesis for the superparticle mass spectrum. A consistent picture is obtained if the lightest superparticle is the gravitino, which can be the dominant component of cold dark matter. In the case of a long-lived charged scalar lepton as next-to-lightest superparticle, supergravity can be tested at the next generation of colliders, LHC and ILC.

Keywords: Baryogenesis, Dark Matter, Big Bang Nucleosynthesis
PACS: 98.80.Cq, 95.35.+d, 12.60.Jv, 95.30.Cq

INTRODUCTION

Leptogenesis [1] is an attractive theory for the origin of matter. Heavy Majorana neutrinos, the seesaw partners of the known light neutrinos, naturally generate a B-L asymmetry in CP violating out-of-equilibrium decays which, via sphaleron processes, is partially converted into a baryon asymmetry. Thermal leptogenesis, where the generated baryon asymmetry is closely related to the light neutrino masses, requires a rather high temperature in the early universe.

In supersymmetric extensions of the standard model, there is a potential clash between the required baryogenesis temperature and the thermal overproduction of gravitinos whose late decays alter the standard predictions of primordial nucleosynthesis (BBN). This leads to strong constraints on the allowed superparticle mass spectrum and, in particular, the allowed lightest superparticle (LSP) [2].

A consistent picture can be obtained in models where the gravitino is the LSP. In a certain mass range for the gravitino and the next-to-lightest superparticle (NLSP) one can avoid the BBN constraints and gravitinos can be the dominant component of dark matter. The NLSP is then quasi-stable, which leads to very interesting effects at colliders [3].

After some comments on the current status of leptogenesis, we discuss in the following the BBN constraints on gravitinos and scalar lepton NLSPs, the perspective for explaining dark matter in terms of gravitinos and some collider signatures.

STATUS OF LEPTOGENESIS

During the past years the theory of leptogenesis has reached a remarkable quantitative state, especially for the simplest scenario where the generation of the baryon asymmetry is dominated by the decays of the lightest of the heavy Majorana neutrinos ('N_1-dominance'). In this case the ratio of baryon density to photon density is determined just by the CP asymmetry ε_1 in N_1 decays, which depends on neutrino masses and mixings,

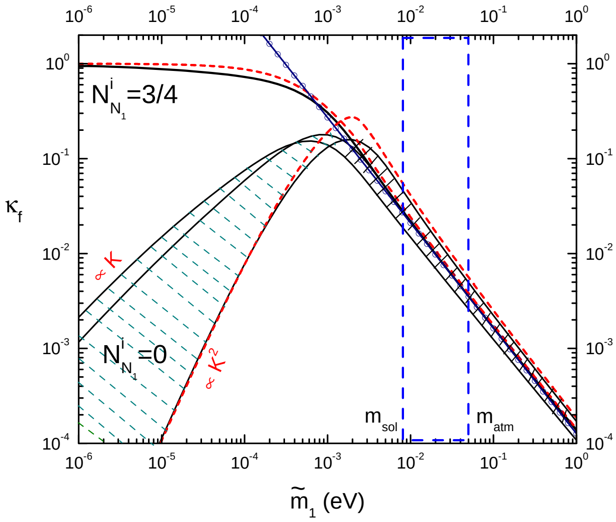

FIGURE 1. The efficiency factor κ_f as function of the effective neutrino mass $\widetilde{m}_1$. From [4].

and the efficiency factor κ_f, which accounts for the dynamics of the non-equilibrium processes in the plasma of the early universe,

$$\eta_B = \frac{n_B}{n_\gamma} \simeq 0.01\,\varepsilon_1\,\kappa_f\ . \tag{1}$$

In Fig. 1 the efficiency factor κ_f is shown as function of the 'effective neutrino mass' $\widetilde{m}_1$ which varies between the smallest and largest light neutrino mass, $m_1 \leq \widetilde{m}_1 \lesssim m_3$. For values below the 'equilibrium neutrino mass', $\widetilde{m}_1 < m_* \simeq 10^{-3}$ eV, the efficiency factor, and therefore the predicted baryon asymmetry has a large uncertainty. Depending on the initial abundance of the heavy neutrinos N_1 and theoretical uncertainties, it varies over several orders of magnitude. On the contrary, for $\widetilde{m}_1 > m_*$, which corresponds to the solar and atmospheric neutrino masses, the value of κ_f is rather accurately determined. In order to avoid too strong lepton-number erasing 'washout processes', the neutrino masses have to obey also the upper bound $m_i < 0.1$ eV. Altogether one then obtains the light neutrino mass window for successful leptogenesis [5]

$$10^{-3}\ \text{eV} < m_i < 0.1\ \text{eV}\ , \tag{2}$$

which will soon be probed by laboratory experiments and cosmological observations. The quantitative analysis of leptogenesis also yields a lower bound on the baryogenesis temperature [6, 4],

$$T_B \sim M_1 \gtrsim 10^9\ \text{GeV}\ , \tag{3}$$

which is very important for the following discussion on gravitino dark matter.

There are several possibilities to avoid the constraints of 'standard thermal leptogenesis' on light neutrino masses and the reheating temperature: the minimal seesaw mechanism can be modified by adding SU(2) triplet fields, one can make use of the enhanced

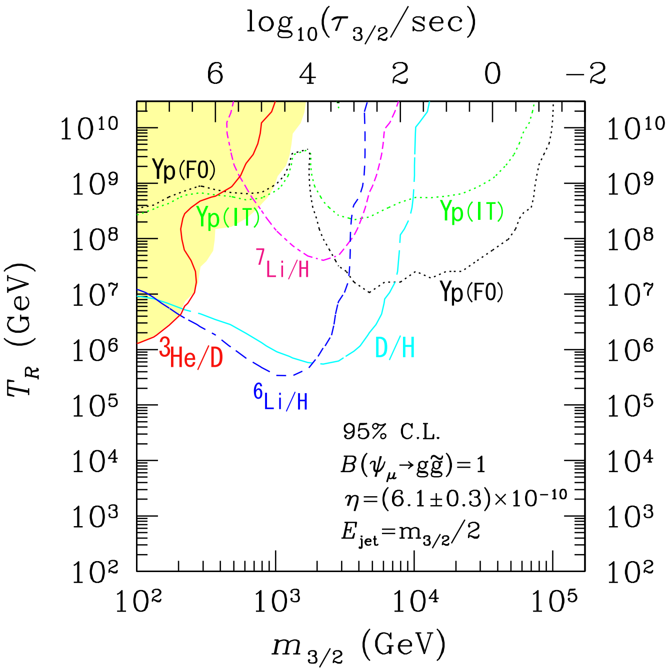

FIGURE 2. Upper bounds on the reheating temperature as function of the gravitino mass. From [9].

CP asymmetry in the case of degenerate heavy neutrino masses (‘resonant leptogenesis’) or one can use non-thermal processes to generate the initial heavy neutrino abundance [2, 7].

An important recent development concerns the detailed study of flavour effects in standard thermal leptogenesis, which can strongly affect the light neutrino mass bound [8]. The constraints on the superparticle mass spectrum follow from the lower bound on the reheating temperature, which is only mildly relaxed by flavour effects.

CONSTRAINTS FROM NUCLEOSYNTHESIS (BBN)

In a supersymmetric plasma at high temperature gravitinos are thermally produced, mostly by QCD processes. Their number density $n_{3/2}$ increases linearly with the reheating temperature,

$$\frac{n_{3/2}}{n_\gamma} \propto \frac{\alpha_3}{M_\mathrm{p}^2} T_R \,, \tag{4}$$

where M_p and α_3 are the Planck mass and the QCD fine structure constant, respectively. The late decay of the gravitinos alters the successful BBN prediction, which implies upper bounds for the reheating temperature T_R. The most stringent one [9] shown in Fig. 2 yields

$$T_R < \mathcal{O}(1) \times 10^5 \text{ GeV} \,, \tag{5}$$

which is clearly incompatible with the lower bound from thermal leptogenesis!

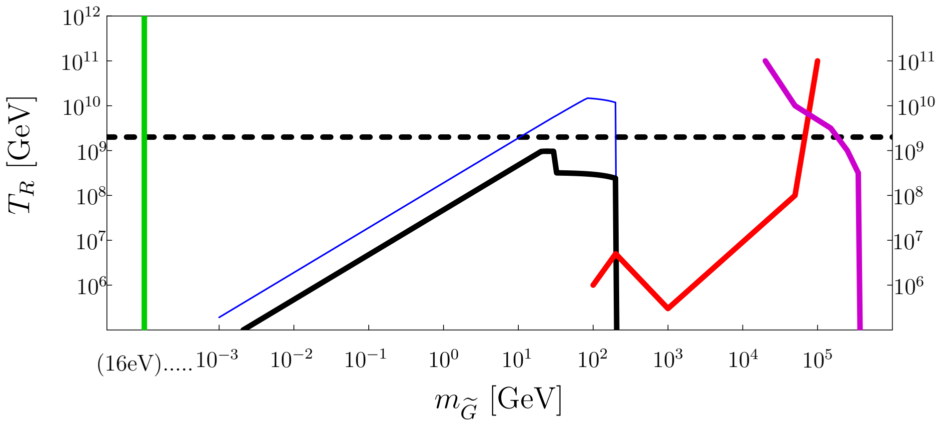

FIGURE 3. Constraints on the reheating temperature from BBN and $\Omega_{\rm CDM}$ as function of the gravitino mass. The dashed line is the lower bound on T_R from leptogenesis. Allowed regions of the gravitino mass are below 16 eV, around 50 GeV and around 10^5 GeV. The blue (black) line corresponds to $m_{\widetilde{g}} = 500$ GeV (1 TeV). The typical gravitino mass $\mathcal{O}(1\ \text{TeV})$ in supergravity models is inconsistent with leptogenesis.

The conflict between the upper bound from BBN and the lower bound from leptogenesis on the reheating temperature can be avoided if the gravitino is the LSP [10]. In this case the BBN bounds apply to the NLSP which is quasi-stable. The gravitino production is now enhanced,

$$\frac{n_{3/2}}{n_\gamma} \propto \frac{\alpha_3}{M_{\rm p}^2}\left(\frac{m_{\widetilde{g}}}{m_{3/2}}\right)^2 T_R\ , \tag{6}$$

where $m_{\widetilde{g}}$ and $m_{3/2}$ are gluino and gravitino mass, respectively. The requirement that the gravitino density does not exceed the observed $\Omega_{\rm DM}$ yields a strong constraint on the reheating temperature for light gravitinos [11]. Cosmological observations constrain very light gravitinos to have masses below 16 eV [12]. BBN and $\Omega_{\rm DM}$ constraints require unstable gravitinos to be extremely heavy [13], $m_{3/2} \sim 10^5$ GeV. The allowed regions for the gravitino mass are summarized in Fig. 3. The BBN constraints for the NLSP have recently been studies by several groups [14, 15]. A neutralino NLSP is excluded, the particularly interesting case of a $\widetilde{\tau}$ NLSP is strongly constrained, and a $\widetilde{\nu}$ NLSP is essentially unconstrained. Recently it has been argued that quasi-stable charged particles alter BBN via the formation of bound states [16, 17]. This could lead to further very restrictive constraints on the allowed NLSP abundance.

The BBN constraints can be weakened by late-time entropy production, i.e., after NLSP decoupling and before BBN. The 'relic' thermal density of $\widetilde{\tau}$'s, $Y_{\widetilde{\tau}}^{\rm thermal} = n_{\widetilde{\tau}}/s$, is then diluted,

$$Y_{\widetilde{\tau}} = \frac{1}{\Delta} Y_{\widetilde{\tau}}^{\rm thermal}\ . \tag{7}$$

This considerably enlarges the parameter region with relatively large gravitino mass, $m_{\widetilde{G}} \geq \mathcal{O}(0.1)\, m_{\widetilde{\tau}}$, which is of particular interest for testing supergravity at colliders. The allowed regions in the $m_{\widetilde{G}}$-$m_{\widetilde{\tau}}$-plane are shown in Fig. 4 for different values of Δ.

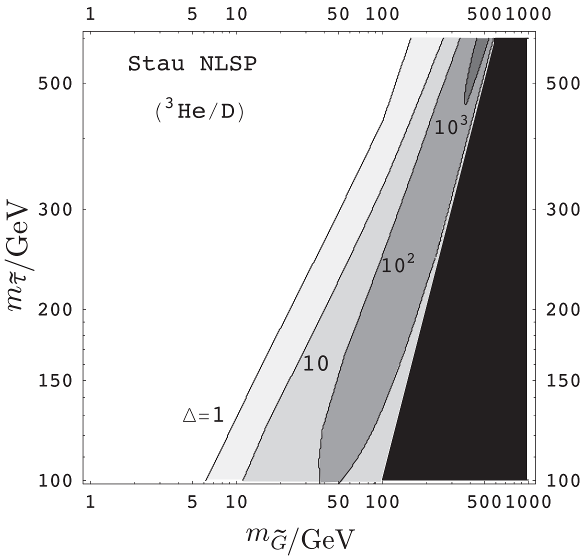

FIGURE 4. The BBN constraint (^{3}He/D bound) on the parameter space $(m_{\tilde{G}}, m_{\tilde{\tau}})$ with late-time entropy production. The regions excluded by the ^{3}He/D bound are shaded from light to dark gray for a dilution factor $\Delta = 1$, 10, 10^2, 10^3. In the black shaded region, the gravitino is not the LSP. The effects of hadronic decays have been neglected. From [18].

GRAVITINO DARK MATTER

So far we have discussed the constraints which the lower bound on the reheating temperature from leptogenesis imposes on the superparticle mass spectrum, and we have argued that the gravitino LSP with an appropriate NLSP represents a consistent scenario. This then leads to the question whether one can understand the observed amount of cold dark matter, $\Omega_{\rm DM}h^2 = \rho_{\rm DM}h^2/\rho_c \simeq 0.11$, in terms of gravitinos, i.e., $\Omega_{\rm DM} \simeq \Omega_{3/2}$.

One possible explanation is the SuperWIMP mechanism [19] where gravitinos are mainly produced in WIMP decays. The gravitino mass density is then determined by the NLSP density,

$$\Omega_{3/2} = \frac{m_{3/2}}{m_{\rm NLSP}}\Omega_{\rm NLSP}\ , \tag{8}$$

which is independent of the reheating temperature T_R! The BBN constraints require, however, a rather large $\tilde{\tau}$ mass, $m_{\tilde{\tau}} > 500$ GeV [14], which makes it difficult to test this mechanism at the next generation of colliders.

Another mechanism is based on the thermal production of gravitinos, which is determined by the Boltzmann equation,

$$\frac{dY_{3/2}}{dT} \propto \frac{\alpha_3(T)}{M_P^2}\frac{m_{\tilde{g}}^2}{m_{3/2}^2}\ . \tag{9}$$

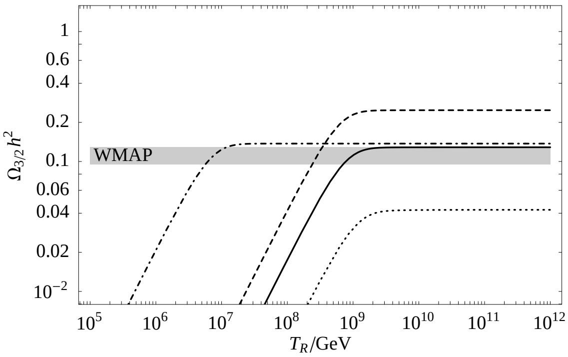

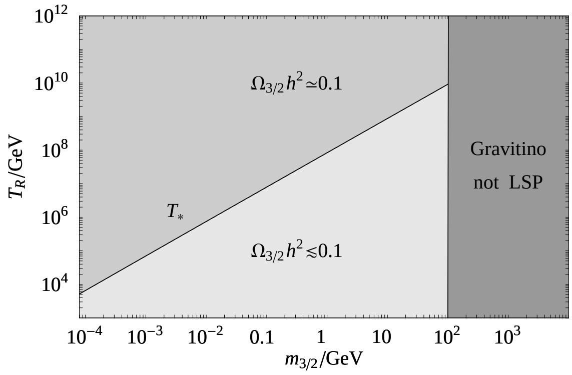

FIGURE 5. Left panel: Relic gravitino density $\Omega_{3/2}h^2$ as function of the reheating temperature T_R for different gravitino and gluino masses: $m_{3/2} = 20$ GeV with $m_{\tilde{g}} = 1.5$ TeV (dashed line), $m_{\tilde{g}} = 1.0$ TeV (full line), $m_{\tilde{g}} = 0.5$ TeV (dotted line), and $m_{3/2} = 200$ MeV with $m_{\tilde{g}} = 1.0$ TeV (dashed-dotted line); $\Omega_{3/2}h^2$ reaches a plateau at $T_R \simeq T_*$. Right panel: Relic gravitino density for different values of reheating temperature and gravitino mass; for $T_R > T_*$, $\Omega_{3/2}h^2$ is independent of T_R and $m_{3/2}$. From [20].

This yields the relic gravitino density

$$\Omega_{3/2}h^2 \simeq 0.2 \left(\frac{T_R}{10^{10}\mathrm{GeV}}\right) \left(\frac{100\mathrm{GeV}}{m_{3/2}}\right) \left(\frac{m_{\tilde{g}}(\mu)}{1\mathrm{TeV}}\right)^2 . \tag{10}$$

It is quite remarkable that the observed CDM density is obtained for typical SUSY breaking parameters, $m_{3/2} \sim 100$ GeV, $m_{\tilde{g}} \sim 1$ TeV and $T_R \sim \sqrt{m_{3/2}M_P} \sim 10^{10}$ GeV.

In general, the relic density of thermally produced gravitinos depends on the reheating temperature, and therefore on the initial conditions in the early universe. There is, however, an interesting case where this dependence disappears. If the gauge coupling depends on a dilaton field, $g = g(\phi)$, as in higher dimensional theories, and the dilaton mass is controlled by supersymmetry breaking, i.e., $m_\phi^2 = \xi m_{3/2}^2$, $\xi = \mathscr{O}(1)$, then the relic gravitino density becomes essentially independent of the reheating temperature as well as the gravitino mass [20].

The gauge coupling multiplies the gauge kinetic term,

$$\mathscr{L}_{eff} = \frac{1}{g^2(\phi)} \left(-\frac{1}{4}F^a_{\mu\nu}F^{a\mu\nu} - i\lambda^a\sigma^\mu(D_\mu\bar{\lambda})^a\right) + \ldots . \tag{11}$$

whose positive expectation value at high temperature drives the effective gauge coupling to smaller values. This effect sets in at a critical temperature

$$T_* \sim \xi^{1/4} \left(\frac{m_{3/2}^2 M_\mathrm{P}}{2m_{\tilde{g}}}\right)^{1/2} , \tag{12}$$

which compensates the increase of the production cross section with temperature. As a consequence, the gravitino production saturates and becomes independent of T above

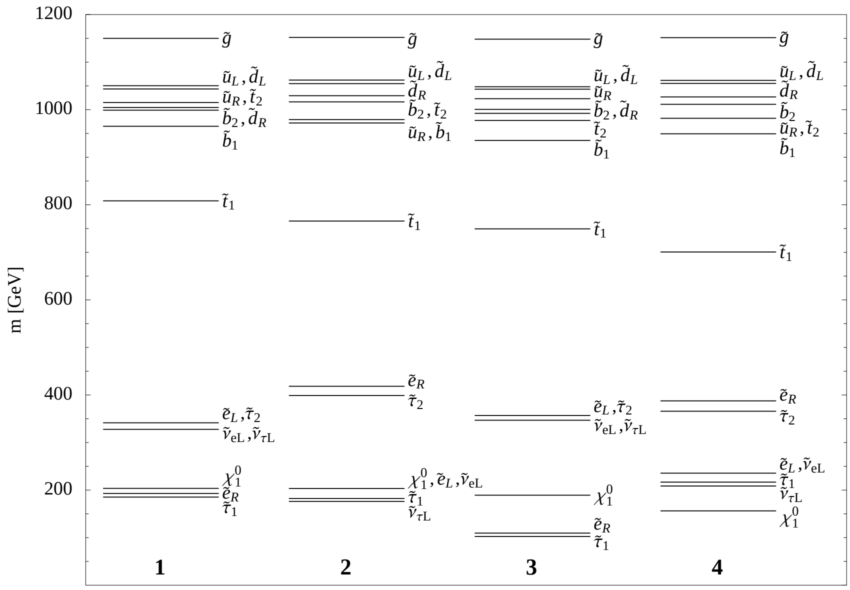

FIGURE 6. Four superparticle mass spectra in gaugino mediation with different NLSP's. From [26].

T_*, yielding

$$\Omega_{3/2}h^2 = 0.1 \times \left(\frac{m_{\tilde{g}}(1\ \mathrm{TeV})}{1\ \mathrm{TeV}}\right)^{3/2} \xi^{1/4} I_{(\alpha)} F(T_*)\ , \tag{13}$$

with the model dependent parameter $I_{(\alpha)}F(T_*) = 0.5\ldots 2$. It is very remarkable that the observed amount of dark matter is obtained for $m_{\tilde{g}} \sim 1$ TeV. A shortcoming of this mechanism is a 'moduli problem', for which so far no fully satisfactory solution has been found.

The described effect of decreasing gauge couplings at high temperatures leads to a simple picture for the generation of matter in the universe. Leptogenesis requires a reheating temperature T_R which is larger than T_* The generated gravitino mass density is then independent of T_R and $m_{3/2}$. The observed value, $\Omega_{3/2} \sim \Omega_{\mathrm{DM}}$, is obtained for $m_{\tilde{g}} \sim 1$ TeV, which will soon be tested at the LHC.

GRAVITINO SIGNATURES AT FUTURE COLLIDERS

How can one detect gravitino dark matter? To distinguish gravitinos from WIMPs in cosmological observations is certainly very difficult! It is therefore encouraging that in the case of a $\tilde{\tau}$-NLSP, the next generation of colliders, LHC and ILC, has the potential to discover the gravitino [21].

Sufficiently slow, strongly ionizing, long-lived $\tilde{\tau}$'s may be stopped. In the 2-body decay $\tilde{\tau} \to \tau\widetilde{G}$ the gravitino mass can then be kinematically determined from $m_{3/2}^2 = m_{\tilde{\tau}}^2 + m_\tau^2 - 2m_{\tilde{\tau}}E_\tau$, with the same accuracy as E_τ and $m_{\tilde{\tau}}$, i.e., a few GeV. Within supergravity, the measurement of the $\tilde{\tau}$-lifetime then yields a determination of the Planck

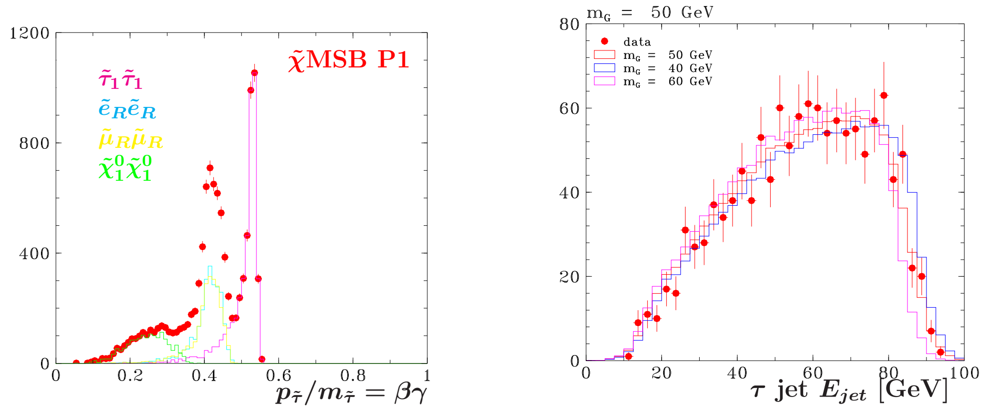

FIGURE 7. Left panel: Momentum spectrum of $\widetilde{\tau}$ leptons. Right panel: τ-jet energy spectrum in $\widetilde{\tau}$ decays. From [24].

mass:

$$M_{\mathrm{P}}^2(\text{supergravity}) = \frac{\left(m_{\widetilde{\tau}}^2 - m_{3/2}^2\right)^4}{48\pi\, m_{3/2}^2\, m_{\widetilde{\tau}}^3 \Gamma_{\widetilde{\tau}}} \,. \tag{14}$$

Agreement with the ‘macroscopic’ Planck mass,

$$M_{\mathrm{P}}^2(\text{gravity}) = (8\pi\, G_{\mathrm{N}})^{-1} = (2.436(2)\cdot 10^{18}\ \text{GeV})^2 \,, \tag{15}$$

would be impressive evidence for supergravity! In more refined experiments it may even be possible to measure the spin of the gravitino. During the past two years several groups have studied the feasibility to test supergravity at LHC and ILC [22, 23].

The gravitino is the LSP in models with gaugino mediated supersymmetry breaking for a wide range of parameters, with a mass $m_{3/2} > 10$ GeV [25]. The NLSP can be either the lighter $\widetilde{\tau}$, the $\widetilde{\nu}$ or a neutralino. Four examples, with different choices of parameters, are shown in Fig. 6 [26]. For the parameter set P1, for instance, one has $m_{\widetilde{\tau}} = 185.2$ GeV and $t_{\widetilde{\tau}} = 9.1\times 10^6$ s for the choice $m_{3/2} = 50$ GeV. Recently, a detailed Monte Carlo study has been carried out for the ILC [23]. Different mass patterns of superparticles have been studied, including the spectrum P1 of gaugino mediation. Several production processes generate $\widetilde{\tau}$'s with the momentum spectrum shown in Fig. 7. For an integrated luminosity $\mathscr{L} \sim 200\ \text{fb}^{-1}$ at $\sqrt{s} = 420$ GeV one expects about 4×10^3 slow ($\beta < 0.3$) $\widetilde{\tau}$'s to be stopped in the hadron calorimeter (HCAL). The $\widetilde{\tau}$ mass and lifetime can be measured rather accurately. From the endpoint of the τ-jet energy the gravitino mass

TABLE 1. Results of a Monte Carlo study for the determination of $m_{\widetilde{\tau}}$, $t_{\widetilde{\tau}}$ and $m_{3/2}$ at the ILC. From [23].

$m_{\widetilde{\tau}}$ [GeV]	$t_{\widetilde{\tau}}$ [s]	$m_{3/2}(\Gamma_{\widetilde{\tau}})$[GeV]	$m_{3/2}(E_\tau)$ [GeV]
185.2 ± 0.1	$(9.1\pm 0.2)\times 10^6$	50 ± 0.6	50 ± 3

$m_{3/2}(E_\tau)$ can be determined with an accuracy of a few GeV. This implies that also the Planck mass can be determined 'microscopically' with an error of about 10% !

In summary, thermal leptogenesis requires a large reheating temperature in the early universe. In supersymmetric theories this leads to strong constraints on the allowed superparticle mass spectrum. The standard supergravity scenario with an unstable gravitino with mass $\mathscr{O}(1 \text{ TeV})$ is imcompatible with thermal leptogenesis. A consistent picture is obtained with a gravitino LSP which can be the dominant component of dark matter. In the case of a $\widetilde{\tau}$ NLSP, the next generation of colliders, LHC and ILC, has the potential to discover the gravitino and to establish spontaneously broken local supersymmetry as a hidden symmetry of nature.

I am grateful to my collaborators on 'leptogenesis and gravitino dark matter', M. Bolz, A. Brandenburg, L. Covi, P. Di Bari, K. Hamaguchi, M. Ibe, J. Kersten, R. D. Peccei, M. Plümacher, M. Ratz, K. Schmidt-Hoberg and T. Yanagida.

REFERENCES

1. M. Fukugita and T. Yanagida, Phys. Lett. **B174**, 45 (1986).
2. For a recent discussion and references, see W. Buchmuller, R. D. Peccei and T. Yanagida, Ann. Rev. Nucl. Part. Sci. **55** (2005) 311.
3. For a recent review and references, see M. Fairbairn et al., arXiv:hep-ph/0611040.
4. W. Buchmuller, P. Di Bari and M. Plumacher, Annals Phys. **315** (2005) 305.
5. W. Buchmuller, P. Di Bari and M. Plumacher, Nucl. Phys. B **665** (2003) 445.
6. S. Davidson and A. Ibarra, Phys. Lett. B **535** (2002) 25.
7. For a review and references, see T. Hambye, arXiv:hep-ph/0412053.
8. T. Endoh et al., Prog. Theor. Phys. **111** (2004) 123; A. Abada et al., JCAP **0604** (2006) 004; E. Nardi et al., JHEP **0601** (2006) 164; A. Abada et al., JHEP **0609** (2006) 010; S. Blanchet et al., arXiv:hep-ph/0607330.
9. M. Kawasaki, K. Kohri and T. Moroi, Phys. Rev. D **71** (2005) 083502.
10. M. Bolz, W. Buchmuller and M. Plumacher, Phys. Lett. B **443** (1998) 209.
11. T. Moroi, H. Murayama and M. Yamaguchi, Phys. Lett. B **303** (1993) 289.
12. M. Viel et al., Phys. Rev. D **71** (2005) 063534.
13. T. Gherghetta et al., Nucl. Phys. B **559** (1999) 27; M. Ibe et al., Phys. Rev. D **70** (2004) 075012.
14. J. L. Feng et al., Phys. Rev. D **68** (2003) 063504; M. Fujii et al., Phys. Lett. B **579** (2004) 6; J. R. Ellis et al., Phys. Lett. B **588** (2004) 7; J. L. Feng et al., Phys. Rev. D **70** (2004) 063514; L. Roszkowski et al., JHEP **0508** (2005) 080; F. D. Steffen, JCAP **0609** (2006) 001; W. Buchmuller et al., arXiv:hep-ph/0609142; T. Kanzaki et al., arXiv:hep-ph/0609246.
15. F. D. Steffen, these proceedings.
16. M. Pospelov, arXiv:hep-ph/0605215; M. Kaplinghat et al., Phys. Rev. D **74** (2006) 103004; R. H. Cyburt et al., arXiv:astro-ph/0608562.
17. K. Kohri and F. Takayama, these proceedings
18. W. Buchmuller, K. Hamaguchi, M. Ibe and T. T. Yanagida, arXiv:hep-ph/0605164.
19. J. L. Feng, A. Rajaraman and F. Takayama, Phys. Rev. Lett. **91** (2003) 011302.
20. W. Buchmuller, K. Hamaguchi and M. Ratz, Phys. Lett. B **574** (2003) 156.
21. W. Buchmuller, K. Hamaguchi, M. Ratz and T. Yanagida, Phys. Lett. B **588** (2004) 90.
22. K. Hamaguchi et al., Phys. Rev. D **70** (2004) 115007; J. L. Feng et al., Phys. Rev. D **71** (2005) 015004; A. Brandenburg et al., Phys. Lett. B **617** (2005) 99; A. De Roeck et al., arXiv:hep-ph/0508198; J. R. Ellis et al., JHEP **0610** (2006) 061.
23. H. U. Martyn, Eur. Phys. J. C **48** (2006) 15.
24. H. U. Martyn, private communication.
25. W. Buchmuller, K. Hamaguchi and J. Kersten, Phys. Lett. B **632** (2006) 366.
26. W. Buchmuller, J. Kersten and K. Schmidt-Hoberg, JHEP **0602** (2006) 069.